

Unifying Short and Long-Term Tracking with Graph Hierarchies

Orcun Cetintas* Guillem Brasó* Laura Leal-Taixé†
 Technical University of Munich, Germany

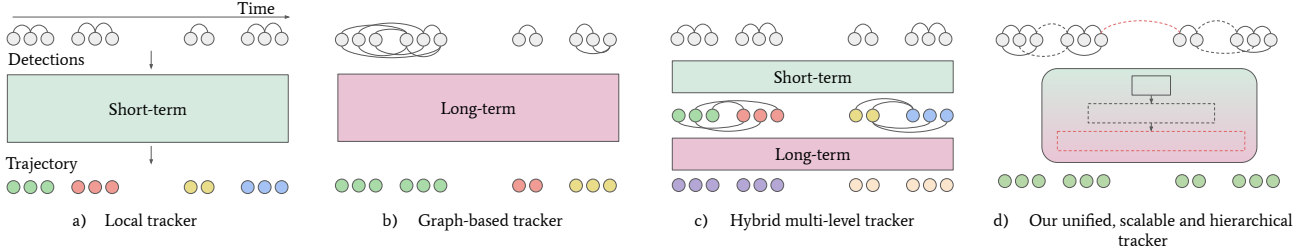


Figure 1. (a) Local tracker focusing on short-term scenarios and lacking robustness at long-term identity preservation (b) Graph-based tracker tackling longer-term association but unable to cover large time gaps due to its limited scalability (c) Hybrid multi-level tracker engineering a combination of techniques but still struggling with scalability (d) Our unified hierarchical tracker with high scalability.

Abstract

Tracking objects over long videos effectively means solving a spectrum of problems, from short-term association for un-occluded objects to long-term association for objects that are occluded and then reappear in the scene. Methods tackling these two tasks are often disjoint and crafted for specific scenarios, and top-performing approaches are often a mix of techniques, which yields engineering-heavy solutions that lack generality. In this work, we question the need for hybrid approaches and introduce SUSHI, a unified and scalable multi-object tracker. Our approach processes long clips by splitting them into a hierarchy of sub-clips, which enables high scalability. We leverage graph neural networks to process all levels of the hierarchy, which makes our model unified across temporal scales and highly general. As a result, we obtain significant improvements over state-of-the-art on four diverse datasets. Our code and models will be made available.

1. Introduction

Multi-Object Tracking (MOT) aims to identify the trajectories of all moving objects from a video. It is an essential task for many applications such as autonomous driving, robotics, and video analysis. Tracking-by-detection is a commonly used paradigm that divides the problem into (i) detecting objects at every frame and (ii) performing data association, i.e., linking objects into trajectories.

In the presence of highly accurate object detections, data

association happens mostly among detections that are close in time, i.e., *short-term association*. Simple cues such as position and motion-based proximity [3, 4, 55, 77, 80] or local appearance [35, 60, 64, 78] are often enough for accurate association. Different challenges appear in crowded scenes, when objects may be often occluded and not detected for several frames. This forces methods to perform association among detections in distant time frames, i.e., *long-term association*. This requires specific solutions that, e.g., build more robust global appearance models [38, 43, 53], create motion models capable of long-term trajectory prediction [12, 23, 45] or bring robustness by performing association across all frames and all trajectories using a graph representation [5, 9, 15, 52, 53].

Due to the different nature of these tasks, solutions used for *short-term* associations tend to fail with *long-term* cases. In fact, most state-of-the-art trackers use a combination of approaches to track over different timespans and therefore can be considered to be *multi-level trackers*. Several short-term trackers use independent re-identification (reID) mechanisms for long-term association [3, 32, 48, 64, 69]. Analogously, various graph approaches rely on local trackers to perform short-term association [5, 17, 18]. All of these *hybrid multi-level* approaches have two main limitations.

The first one is **scalability** since current methods cannot deal directly with long videos. As we increase the timespan between detections to be linked, association becomes more ambiguous due to the possibility of significant appearance changes and large displacements. Hence, local trackers using a handcrafted combination of appearance and motion cues will fail to scale to arbitrary timespans. Graph-based methods are more robust, but association for large

* Equal contribution.

† Currently at NVIDIA.

timespans entails the creation of very large graphs (even when combined with local methods), which is infeasible both computationally and memory-wise.

The second limitation is **generality**. Using different techniques for different timespans requires making strong assumptions about the cues needed at each temporal scale, which limits the applicability of these approaches. For instance, in tracking scenarios where people dress uniformly and frame rate is high, e.g. dancing videos [50], proximity or motion-based local trackers [3, 4, 77, 80] are more reliable than appearance-based trackers. On the other hand, in the presence of heavy camera motion or low frame rates, the performance of the aforementioned trackers degrades significantly, and appearance may become the most reliable cue [35, 72]. Overall, these discrepancies lead inevitably to handcrafted solutions for each type of scenario.

In this work, we ask the following question: *can we design a unified method that generalizes to multiple timespans and further scales to long videos?*

We propose a method that processes videos hierarchically: lower levels of our hierarchy focus on short-term association, and higher levels focus on increasingly long-term scenarios. The key differences to existing *hybrid* multi-level solutions is that we use *the same learnable model* for all time scales, i.e., hierarchy levels. Instead of hand-crafting different models for different scales, we show that our model can learn to exploit the cues that are best suited for each time-scale in a data-driven manner. Furthermore, our hierarchy allows a finer-grained transition from short to long-term instead of using two distinct stages. Our method targets the two main limitations of previous works: (i) its hierarchical structure makes it highly scalable and enables processing long clips efficiently, and (ii) it is highly general and does not make any assumptions about which cues are best suited for which timespans, but instead allows the model to obtain the necessary cues in a data-driven manner. We, therefore, obtain a **Strong** tracker, with a **Unified** solution across timespans, and good **Scalability** thanks to its **Hierarchical** nature, and name it **SUSHI**.

At its core, SUSHI is a graph method, but instead of working on a single monolithic graph, we embrace the different nature of data association over different timespans and operate on a hierarchy of smaller graphs. At the lowest level of our hierarchy, nodes represent object detections in nearby frames. We use a graph neural network (GNN) [5, 14, 47] to process those into short tracklets, and then build new graphs to generate increasingly longer trajectories at every level of our hierarchy. Notably, we use *the same GNN architecture at every level*. Thus we do not make any assumptions about what cues are the best for each timespan.

We demonstrate the generality of our approach by showing significant identity preservation improvements over

the state-of-the-art in several highly diverse benchmarks. Namely, we achieve improvements of up to **+3** IDF1 on MOT17 [10], **+5.7** IDF1 on MOT20 [11], **+6.8** IDF1 on DanceTrack [50], and **+3.1** IDF1 on BDD [72] over previous work, therefore setting new state-of-the-art results by a significant margin. We will release our code and models.

2. Related Work

Short-term tracking. Numerous modern trackers use frame-by-frame online association frameworks [3, 4, 32, 35, 55, 60, 67, 74, 77, 78, 80]. Motion and spatial proximity cues tend to be central components of these trackers. Notable examples include the widespread use of kalman-filter based motion models [4, 60, 77, 78] or frame-by-frame regression-based frameworks [3, 32, 74, 80]. Some trackers further rely on appearance to increase robustness at lower frame-rates or under strong camera movement [35, 60, 64, 67, 78]. While having good performance in short-term scenarios, these trackers lack robustness when it comes to long-term identity preservation.

Graph-based tracking. Graphs are a commonly used framework to model data association. They model nodes as object detections and edges as trajectory hypotheses. In contrast to frame-by-frame trackers, graph-based methods search for *global* solutions to the data association problem over several frames and are therefore most robust. To this end, numerous optimization frameworks have been studied, including network flows [2, 76], multi-cuts [53], minimum cliques [73], disjoint paths [17, 18, 52], and have designed efficient solvers for them [2, 6]. In our work, we rely on a simplified version of the min-cost flow formulation [5, 76], which allows us to avoid expensive optimization and use a small-scale linear program, while still taking advantage of graph-based tracking.

Learning in graph-based tracking. While early graph-based methods focused on obtaining pairwise association costs from learning methods such as conditional random fields [71], or handcrafted models [51], recent approaches focus almost exclusively on deep learning techniques. Notable examples include learning pairwise appearance costs with convolutional networks [22, 44, 48], or learning track management policies with recurrent models [33, 46]. Recently, numerous approaches learn models that natively operate on the graph domain such as graph neural networks (GNNs) [5, 9, 15, 25, 30, 63] or transformers [81]. While promising, current GNN and transformer-based works have an important limitation: they operate over large monolithic graphs of detections, and therefore lack the scalability needed to process long video clips.

Multi-level hybrid tracking approaches. Multi-level tracking methods are dominated by handcrafted combinations of approaches. Several early tracking works exploited the idea of building tracks hierarchically [8, 19, 62, 68]. They

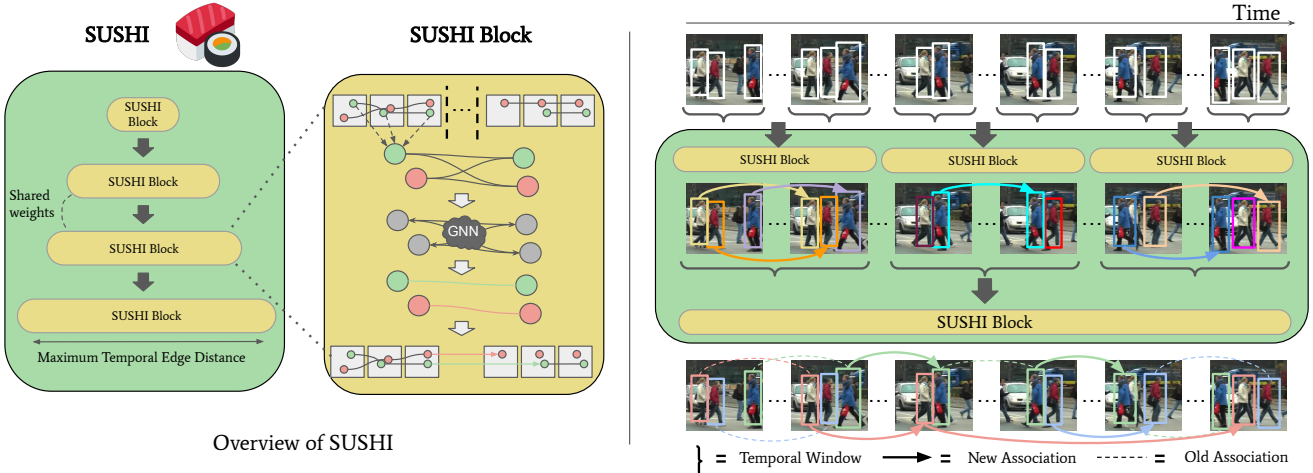


Figure 2. SUSHI consists of a set of SUSHI blocks operating hierarchically over a set of tracklets (with initial length one) in a video clip. Each SUSHI block considers a graph with tracklets from a subclip as nodes, performs neural message passing over it, and merges nodes into longer tracks. Over several hierarchy levels SUSHI blocks are able to progressively merge tracklets into tracks spanning over the entire clip. Notably, *all SUSHI blocks share the same GNN architecture and weights*, hence making SUSHI unified across temporal scales.

generally did so by generating short tracklets with hand-crafted methods and then merging those within multiple stages involving different optimization techniques [8, 62, 68], and association cues [19]. In the case of modern trackers, a significant portion of them still relies on a combination of techniques [3, 5, 9, 17, 18, 32, 65]. Some examples include short-term trackers using external networks for reID-based association [3, 32, 64], and graph-based methods relying on local trackers to either generate tracklets [5] or fill gaps in trajectories [17, 18]. In our work, we show that we do not need to manually combine techniques, and instead, we use a unified GNN-based framework to efficiently perform data association across multiple hierarchical levels.

3. Background

Tracking by detection. Our approach follows the *tracking-by-detection* paradigm. That is, given a video clip, we assume that object detections are computed for every frame, and our task is to perform data association by linking object detections into trajectories. We denote the set of object detections as \mathcal{O} . Each object detection $o_i \in \mathcal{O}$ can be identified by its bounding box coordinates, its corresponding image region, and timestamp. The goal of the data association step is to obtain the set of trajectories \mathcal{T}^* that group detections corresponding to the same identity. Each trajectory T_k is given by its set of detections $T_k := \{o_{k_i}\}_{i=1}^{n_k}$, with n_k being the number of object detections, or trajectory length.

Graph-based tracking. Our method builds on the commonly used graph-based formulation of [76], which we briefly review. We model data association with an undirected graph $G = (V, E)$ in which each node corresponds

to an object detection, *i.e.*, $V := \mathcal{O}$. Edges represent association hypotheses among objects at different frames $E \subset \{(o_i, o_j) \in V \times V | t_i \neq t_j\}$. Formally, a time-ordered track $T_k = \{o_{k_i}\}_{i=1}^{n_k}$ with $t_{k_i} < t_{k_{i+1}}$, can be represented as a path in G given by its edges $E(T_k) := \{(o_{k_1}, o_{k_2}), \dots, (o_{k_{n_k-1}}, o_{k_n})\}$. Therefore, edges $(u, v) \in E$ can be classified into correct hypotheses if $(u, v) \in E(T_k)$ for some $T_k \in \mathcal{T}^*$, in which case we denote $y_{(u,v)} = 1$; or incorrect otherwise, *i.e.* $y_{(u,v)} = 0$. Given a set of edge predictions or *costs*, $\{y_{(u,v)}^{\text{pred}}\}_{(u,v) \in E}$ aiming to estimate the set of edge labels $\{y_{(u,v)}\}_{(u,v) \in E}$, final trajectories can be obtained by rounding predictions into binary decisions via discrete optimization or heuristics, and then extracting their corresponding paths in the graph. Overall, this formulation allows casting data association as an edge labeling task.

4. SUSHI

We provide an overview of SUSHI in Fig. 2. It consists of a sequence of jointly trained *SUSHI blocks* that operate over a video clip. Starting from initial per-frame object detections (referred to as tracklets of length one from now on) each SUSHI block learns to merge tracklets from the previous level into longer ones. To do so, each SUSHI block builds a graph in which the nodes represent tracklets from the previous level and the edges model trajectory hypotheses. Nodes and edges have associated embeddings encoding position, appearance, and motion cues that are propagated across the graph with a GNN. After several message-passing steps, edge embeddings are classified into correct and incorrect hypotheses, yielding a new set of longer tracklets. By hierarchically stacking several SUSHI

blocks, tracklets grow progressively into our final output: final tracks spanning over the entire input video clip.

Overall, the GNN in each SUSHI block learns to exploit timespan dependent association cues, and combined, SUSHI blocks enable tracking over long-time horizons efficiently.

4.1. Constructing a hierarchy of tracking graphs

On the limitations of monolithic tracking graphs. Given an input video clip with C frames, our goal is to enable the association of objects even if they are occluded for long time spans, i.e., up to $C - 1$ frames. Given the graph formulation we introduced in Sec. 3, this is only possible if we consider edges in our graph spanning across all possible time distances. Doing so naively has two main drawbacks. First, it is prohibitively expensive for long sequences, as it requires either considering a quadratic number of edges or using sophisticated pruning techniques. Secondly, it implies that most edges in the graph will represent incorrect hypotheses. To prove that, observe that each object detection can, at most, be incident to two correct edges (one in the past, and one in the future). Therefore, in a clip with n object detections, the correct number of hypotheses is at most $2n$, while the number of edges can grow up to n^2 . The ratio $o(\frac{1}{n})$ will vanish for sequences consisting of thousands of detections and will cause a severe label imbalance for learning methods operating on those edges.

Building a hierarchical clip partition. Motivated by the aforementioned limitations, we propose a hierarchy of smaller graphs that operate over long video clips instead of a single large monolithic graph. Our hierarchy is based on a recursive partition of the clip into non-overlapping time windows or smaller clips. We illustrate our construction in Figure 3. At each consecutive hierarchy level we only consider edges among tracklets contained in small windows of consecutive frames, which ensures that our tracklet length is relatively uniform at every level. After each consecutive level in our hierarchy, we merge tracklets that are close in time into longer ones. These longer tracklets then become our new set of nodes to be associated at the following hierarchy level. By recursively merging tracklets in nearby frames, we progressively reduce the number of nodes after each hierarchy level. Therefore, at each consecutive level of our hierarchy, we can consider edges spanning across longer timespans without neither prohibitively increasing the edge count, nor incurring a severe label imbalance.

4.2. Learning a unified hierarchical tracker

Overview. In the previous section, we presented a hierarchical graph-based framework to recursively merge short tracklets into longer ones. We use a message-passing GNN to process graphs in our hierarchy and learn to merge tracklets. We refer to each hierarchical module of our model as

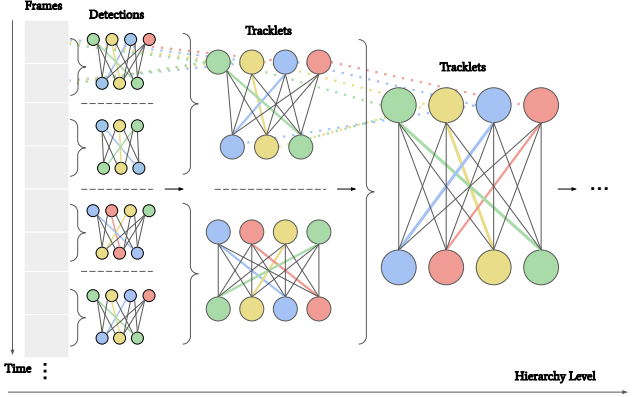


Figure 3. Our hierarchy is based on recursive partitioning of the video clip and we only allow edges within these partitions. After each level, we merge tracklets belonging to the same identity and consider edges spanning across longer timespans.

a *SUSHI block*. A core feature of our method is that each SUSHI block uses the same architecture, and has access to the same feature sources. This is in contrast to previous work that engineered different solutions for different levels [5, 9, 17, 18]. Therefore, we do not make any assumptions on the cues needed to perform association at each timespan and instead, let SUSHI blocks at each hierarchy *learn* these from data.

SUSHI blocks. An illustration of a SUSHI block is shown in Figure 2. Inspired by [5], the main idea behind them is: (i) consider a graph with tracklets as nodes as defined in Section 4.1, (ii) propagate node and edge embeddings across the graph via message-passing, and (iii) perform edge classification to merge nodes, i.e., tracklets, into longer tracklets. More specifically, for each graph $G^l = (V^l, E^l)$ at level l in our hierarchy, we consider embeddings $h_v^{(0)} \in \mathbb{R}^{d_V}$ and $h_{(u,w)}^{(0)} \in \mathbb{R}^{d_E}$ for every node $v \in V^l$ and edge $(u, w) \in E^l$, with d_V and d_E being their respective dimension. Node embeddings are zero-initialized, and edge embeddings are learned from a set of initial association features. The goal of message-passing is to then propagate embeddings across the graph, hereby encoding higher-order contextual information in them. To do so, we follow the time-aware neural message-passing framework of [5] for $s = 1, \dots, S$ steps, yielding embeddings $h_{(u,v)}^{(1)}, \dots, h_{(u,v)}^{(S)}$. After the last step, edge embeddings are fed to a binary classifier to obtain a score representing whether they represent a correct hypothesis or not, $y_{(u,v)}^{\text{pred}} = \text{MLP}_{\text{class}}(h_{(u,v)}^{(S)})$. After that, predicted edge scores are rounded to obtain binary decisions using a linear program. As an end result, we obtain a longer-spanning set of tracklets from the initial ones in V^l . Further details on our GNN and rounding scheme are provided in the supplementary material.

Edge association cues. We compute input edge embeddings to the GNN in each SUSHI block by feeding an initial vector of concatenated pairwise association features to a light-weight multi-layer perception MLP_{edge} . The initial vector computation is a generalization and extension of that of [5] to tracklets and considers the spatial and motion-based proximity, time distance, and reID embedding-based appearance similarity between nodes. For appearance, we consider the average embedding vector over all detections in the tracklet which is more robust than that of a single detection. For spatial, size, and time proximity, we use the closest detections in time for each pair of nodes. Explicitly working with tracklets allows us to utilize motion, a strong cue that [5] does not exploit. We add a motion component to initial edge embeddings by computing the Generalized IoU [39] of the forward and backward propagated positions by a linear motion model for every pair of tracks. For further details, we refer to the supplementary material.

Weight sharing. SUSHI blocks use the same GNN architecture at every hierarchy level. We observe that we can *share parameters and learnable weights* among the GNNs used for each SUSHI block. To do so, we additionally learn a level embedding ϕ_l for each level l in our hierarchy. Level embeddings are added to the output edge embeddings produced by MLP_{edge} , and allow edge embeddings to encode the specific feature differences to be expected at each hierarchy level (e.g. larger time distances or spatial displacements at higher levels). By sharing weights among levels, we boost the number of training samples that our GNNs have, as they now can benefit from data from multiple hierarchy levels. Empirically, we observe improved performance and convergence speed, together with a reduction in overall parameter count.

Training. Our message-passing GNNs are trained jointly across all levels. To do so, we sequentially unfreeze levels from first to last. This ensures that tracklets used in each subsequent level in the hierarchy during training are stable and accurate enough to provide a meaningful signal. Specifically, starting with only the first block being unfrozen, we unfreeze each subsequent level after M training iterations, with $M = 750$ in our implementation. After the GNNs from all levels are unfrozen, they are trained jointly. This allows them to adapt to the particular tracklet statistics produced by their predecessors. For each level, we use a focal loss [29] over the classification scores produced over the edges, and sum losses over all levels to obtain our final loss.

5. Experiments

5.1. Datasets and Metrics

We conduct experiments on four public benchmarks with significantly different properties: MOT17 [10], MOT20 [11], DanceTrack [50], and BDD100K [72].

MOT17. The benchmark includes diverse scenarios with varying camera viewpoints and pedestrian densities. It consists of 14 videos (7 for training, and 7 for testing) with a total of 11235 frames. In the public setting, object detections are provided to emphasize data association performance during evaluation. In contrast, in the private setting trackers are allowed to use their own set of detections.

MOT20. The dataset focuses on extremely crowded scenes, with some videos containing over 200 pedestrians per frame on average. It contains 8 videos (4 for training and 4 for validation), and a total of 13410 frames with more than 2 million object annotations. Similarly to MOT17, it considers public and private settings separately.

DanceTrack. The dataset consists of group dancing videos (100 videos and 105855 images). Scenes in the dataset are moderately crowded and contain persons with highly similar appearances and complex and diverse motion patterns.

BDD100K. The dataset focuses on egocentric vision from a car-mounted camera in highly diverse autonomous driving scenarios. Due to the nature of the task, large camera motion is prominent. The MOT benchmark contains 2,000 videos with approximately 400K images and 8 object categories are annotated for evaluation.

Metrics. To evaluate several aspects of MOT, we report the widely accepted metrics IDF1 [40], MOTA [20], and recently introduced HOTA [31]. While IDF1 measures identity preservation, MOTA is heavily biased towards trajectory coverage, i.e., detection quality. HOTA finds balance between both aspects, and unifies association and localization performance into a single metric. Since our method focuses on data association, we treat IDF1 and HOTA as main metrics, and also report MOTA and identity switches (ID Sw.) for completeness.

5.2. Implementation Details

Model architecture and training. SUSHI consists of four SUSHI blocks utilizing MPNTrack [5]’s GNN architecture and shared weights between hierarchy levels. For our reID feature extractor we use a pretrained ResNet50-IBN following [9]. We do not fine-tune our reID model on tracking videos, and simply freeze it during training. GNNs across hierarchical levels are trained jointly with a learning rate of $3 \cdot 10^{-4}$ and a weight decay of 10^{-4} in batches of 8 clips for 100 epochs. We use focal loss with $\gamma = 1$ and the Adam optimizer [21].

Hierarchy construction and inference. Though our model is capable of processing sequences of arbitrary length, we construct hierarchies spanning a maximum temporal edge distance of 150 frames (approx. 6-10 seconds on MOT17). We experimentally found that this covers the majority of long-term association cases across multiple datasets, and is a significant improvement over previous works, which processed clips of up to 15 [5], 32 [81], and 60 frames [17, 18].

Method	Short Term (≤ 25 Frames)	Long Term (75 Frames)	Long Term++ (150 Frames)	IDF1	HOTA	MOTA		
IoU	IoU	\times	\times	60.5	55.4	64.9		
Tracktor	Reg.	\times	\times	65.6	58.9	66.0		
IoU++	IoU	ReID + Motion	\times	65.1	58.4	65.8		
Tracktor++	Reg.	ReID + Motion	\times	69.2	60.7	66.8		
MPNTrack	Reg.	GNN	\times	71.8	62.8	67.6		
MPNTrack++	Reg.	GNN †	\times	73.2	62.9	67.7		
SUSHI (Ours) - 2 Level	Hierarchy of 2 GNN †		\times	73.5	63.8	67.7		
Tracktor++	Reg.	ReID+Motion		71.2	62.5	66.4		
MPNTrack	Reg.	GNN		71.9	62.8	67.6		
MPNTrack++	Reg.	GNN †		73.4	63.7	68.0		
SUSHI (Ours) - 2 Level	Hierarchy of 2 GNN †			73.8	64.2	68.3		
SUSHI (Ours)	Hierarchy of 4 GNN †			76.0	65.8	68.6		

Table 1. Ablation study on hybrid and unified multi-level approaches.

Our hierarchy consists of four levels, each processing sub-clips of 5, 25, 75 and 150 frames, respectively. For each graph, we connect each node to its top 15 nearest neighbors based on geometry, appearance, and motion similarity. We process entire videos by feeding overlapping clips of 150 frames to our method in a sliding window fashion. We then merge per-clip tracks into trajectories of arbitrary length with a simple stitching scheme, similarly to [5]. During inference, we fill trajectory gaps by linear interpolation.

Runtime. Inference runs at a competitive runtime of 24fps on MOT17 and 10fps on the heavily crowded sequences of MOT20, with given detections.

Object Detections. For DanceTrack and BDD, as well as the private settings of MOT17 and MOT20, we obtain object detections from a YOLOX detector [13] trained following [77]. In the public setting of MOT17 and MOT20, for a fair comparison to the state-of-the-art, we use the public detections provided by MOTChallenge and preprocess them with [3] following [5, 9, 15, 17].

5.3. Ablation Studies

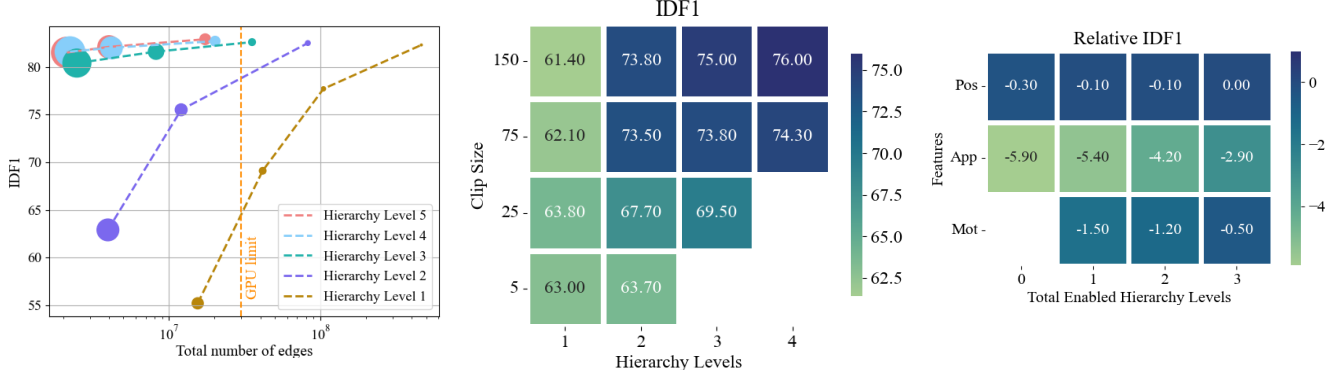
We conduct the ablation experiments on the MOT17 train set by performing 3-fold cross-validation following [5]. Our ablation studies analyze two main aspects of our method: (i) the advantages of using a unified method across different levels of our hierarchy for data association, and (ii) our model’s ability to scale to long video clips.

Hybrid vs unified multi-level approaches. In Table 1 we analyze the performance differences between hybrid multi-level approaches and our unified GNN-based approach. We consider three association time horizons of up to 25, 75, and 150 frames, and analyze the strengths of each approach at each time horizon. We initially consider two local baselines: a framewise hungarian matching tracker (IoU), and a superior regression-based tracker (Tracktor) [3]. As addi-

tional baselines, we add long-term association levels using a combination of reID and motion cues (IoU++, Tracktor++). We observe that single-level GNNs show stronger performance at this second level (MPNTrack, MPNTrack++¹), and using GNNs at both levels achieves the best performance gains at up to 75 frames. This shows that the benefits of being a unified method are also applicable at moderate timespans of up to 75 frames. In the penultimate four rows, we attempt to naively extend hybrid approaches to perform association over longer time horizons of up to 150 frames, and observe no significant improvements, due to the increased difficulty of these scenarios. In contrast, our four-level hierarchy benefits from tracking over increased timespans. In the following paragraphs, we investigate the reasons behind the need for additional hierarchy levels.

The potential of hierarchies over monolithic graphs. As explained in Sec. 4.1, our graph hierarchy allows us to cover large time spans with a significantly reduced number of edges, while mitigating the label imbalance between correct and incorrect trajectory hypotheses. To quantify this phenomenon, we compute the oracle IDF1 score, i.e., assuming perfect edge classification, of models consisting of a varying number of hierarchical levels over video clips of 150 frames. In Fig. 4a, we report both the overall number of edges needed to achieve each score, and the corresponding ratio of correct edge hypotheses, i.e., labels, encoded as the circle area. For each number of levels (color-coded) each of its data points is obtained by changing the number of nearest neighbors of nodes. We observe a clear trend: hierarchical graphs achieve significantly higher scores for a fixed memory budget. At the same time, they do so with a significantly less severe label imbalance, i.e., a larger circle

¹The difference between MPNTrack and MPNTrack++ is the use of motion features within initial edge embeddings, which were not exploited in MPNTrack [5] and we denote as GNN † .



(a) Potential of hierarchies over monolithic graphs. (b) Effect of clip length and hierarchy levels. (c) Importance of features at different levels.

Figure 4. Ablation studies on scalability of our approach and association cues.

area, which indicates that learning on them will be significantly easier. It is important to note that the benefits of our hierarchy saturates after four hierarchy levels, and therefore we use this value in our model. Overall, Fig. 4a, highlights the main two reasons behind the scalability of our hierarchy.

Method	Det Ref.	IDF1 \uparrow	HOTA \uparrow	MOTA \uparrow	ID Sw. \downarrow
MOT17 - Public					
Tracktor [3]	Tracktor	55.1	44.8	56.3	1987
LPT [27]	Tracktor	57.7	—	57.3	1424
MPNTrack [5]	Tracktor	61.7	49.0	58.8	1185
Lif_T [17]	Tracktor	65.6	51.3	60.5	1189
ApLift [18]	Tracktor	65.6	51.1	60.5	1709
GMT [15]	Tracktor	65.9	51.2	60.2	1675
LPC_MOT [9]	Tracktor	66.8	51.5	59.0	1122
SUSHI (Ours)	Tracktor	68.6	53.0	62.2	1062
MOT17 - Private					
QDTrack [36]	✗	66.3	53.9	68.7	3378
TrackFormer [32]	✗	68.0	57.3	74.1	2829
MOTR [75]	✗	68.6	57.8	73.4	2439
PermaTrack [55]	✗	68.9	55.5	73.8	3699
MeMOT [7]	✗	69.0	56.9	72.5	2724
GTR [81]	✗	71.5	59.1	75.3	2859
FairMOT [78]	✗	72.3	59.3	73.7	3303
GRTU [58]	✗	75.0	62.0	74.9	1812
CorrTracker [57]	✗	73.6	60.7	76.5	3369
Unicorn [70]	✗	75.5	61.7	77.2	5379
ByteTrack [†] [77]	✗	77.1	62.8	78.9	2363
ByteTrack [77]	✗	77.3	63.1	80.3	2196
SUSHI (Ours)	✗	80.5	65.2	80.7	1335

Table 2. Test set results on MOT17 benchmark. Det. Ref. denotes the public detection refinement strategy. As ByteTrack (gray) uses different thresholds for test set sequences and interpolation, we also report scores by disabling these as ByteTrack[†] (black).

Effect of clip length and hierarchy levels. In Fig. 4b, we visualize the impact on identity preservation (IDF1) when we increase the number of hierarchy levels and the clip

length, hence incorporating longer-term association scenarios. As explained in the previous paragraph, increasing the clip size allows the tracker to potentially bridge longer occlusions, but a naive increase in size yields a very large graph with severe label imbalance. This is confirmed in the first column of Fig. 4b: increasing the clip length in a non-hierarchical way, i.e., using a single level, can even harm performance when going beyond moderate lengths (≥ 25 frames). Conversely, given a fixed clip size, increasing the number of hierarchy levels up to four yields monotonic improvements for all clip lengths. Overall, our hierarchical framework enables processing clip sizes of up to 150 frames, with an overall improvement of +12.2 IDF1 over a naive, i.e., single level, baseline.

Importance of features at different levels. As explained in Sec. 4.2, our GNNs exploit three main feature modalities: position, appearance, and motion. In Fig. 4c, we show the ability of our networks to utilize association cues differently at each hierarchy level, that is, over different association timespans. To do so, we report the performance loss obtained from removing edge features from each type over individual levels. Starting from completely removing features from each modality while keeping other modalities intact (first column), we add features of the target type sequentially over consecutive layers. We observe that appearance has the largest impact, but it is mostly used at later hierarchy levels since adding it at the first level only yields a minor 0.5 IDF1 improvement. Motion seems to have a moderate but uniform impact across levels, and lastly, position information is only relevant for short-term association.

5.4. Benchmark Results

MOT17. Under the public setting, our model outperforms all published work using Tracktor-based preprocessing (Table 2). It is worth noting that all listed methods are graph-based and our approach significantly surpasses their identity preservation performance, as measured by IDF1 and HOTA.

Compared to MPNTrack, we achieve an improvement of 6.9 IDF1 and 4.0 HOTA, despite using their GNN architecture in our SUSHI blocks, which highlights the importance of our graph hierarchy. Analogously, we also obtain significant improvements over hybrid graph-based methods [9, 17, 18]. In the private setting, we significantly improve upon all published methods. While using the same detector as ByteTrack [77], our model improves upon it by 3.2 IDF1 and 1.9 HOTA, and reduces ID switches by 40%.

Method	Det Ref.	IDF1 \uparrow	HOTA \uparrow	MOTA \uparrow	ID Sw. \downarrow
MOT20 - Public					
Tracktor [3]	Tracktor	52.7	42.1	52.6	1648
LPT [27]	Tracktor	53.5	—	57.9	1827
ApLift [18]	Tracktor	56.5	46.6	58.9	2241
MPNTrack [5]	Tracktor	59.1	46.8	57.6	1210
LPC_MOT [9]	Tracktor	62.5	49.0	56.3	1562
SUSHI (Ours)	Tracktor	68.2	53.4	61.6	1078
MOT20 - Private					
TrackFormer [32]	X	65.7	54.7	68.6	1532
MeMOT [7]	X	66.1	54.1	63.7	1938
FairMOT [78]	X	67.3	54.6	61.8	5243
GSDT [59]	X	67.5	53.6	67.1	3131
CorrTracker [57]	X	69.1	—	65.2	5183
ByteTrack † [77]	X	74.5	60.4	74.2	925
ByteTrack [77]	X	75.2	61.3	77.8	1223
SUSHI (Ours)	X	77.7	63.1	74.3	704

Table 3. Test set results on MOT20 benchmark. Det. Ref. denotes the public detection refinement strategy. As ByteTrack (gray) uses different thresholds for test set sequences and interpolation, we also report scores by disabling these as ByteTrack † (black).

MOT20. In the crowded and challenging scenes of MOT20, we achieve even greater improvements over previous work, which further highlights the scalability benefit of our hierarchical and unified framework (Table 3). In the public setting, we surpass all state-of-the-art approaches, remarkably, by 5.7 IDF1 and 4.1 HOTA while, again, using the same refinement model over public detections. In the private setting, we also advance the state-of-the-art by 2.4 IDF1 and 1.8 HOTA, while again significantly reducing ID switches.

DanceTrack. In Table 4, we report a remarkable improvement of 6.8 IDF1 and 7.1 HOTA over state-of-the-art. Given the unique features of this dataset, these results highlight the versatility of our approach to utilize the right cues for different scenarios. This is in contrast with methods like [77] that show strong performance in HOTA at both MOT17 and MOT20, but fall behind other approaches on Dance-track. Our improvements are consistent across datasets, which demonstrates the generality of SUSHI.

BDD. We further demonstrate the versatility of our approach in Table 5 where we report results on the highly diverse BDD. Note that this dataset contains multiple classes,

Method	IDF1 \uparrow	HOTA \uparrow	MOTA \uparrow	AssA \uparrow	DetA \uparrow
DanceTrack					
CenterTrack [80]	35.7	41.8	86.8	22.6	78.1
FairMOT [78]	40.8	39.7	82.2	23.8	66.7
TraDes [66]	41.2	43.3	86.2	25.4	74.5
GTR [81]	50.3	48.0	84.7	31.9	72.5
QDTrack [35]	50.4	54.2	87.7	36.8	80.1
MOTR [75]	51.5	54.2	79.7	40.2	73.5
ByteTrack [77]	53.9	47.7	89.6	32.1	71.0
SUSHI (Ours)	60.7	61.3	89.9	46.8	80.5

Table 4. Test set results on DanceTrack benchmark.

Method	mIDF1 \uparrow	mMOTA \uparrow	IDF1 \uparrow	MOTA \uparrow	ID Sw. \downarrow
BDD - Validation					
MOTR [75]	43.5	32.0	—	—	—
Yu <i>et al.</i> [72]	44.5	25.9	66.8	56.9	8315
QDTrack [35]	50.8	36.6	71.5	63.5	6262
TETer [26]	53.3	39.1	—	—	—
Unicorn [70]	54.0	41.2	71.3	66.6	10876
ByteTrack [77]	54.8	45.5	70.4	69.1	9140
SUSHI (Ours)	57.5	46.0	75.2	69.1	7283
BDD - Test					
Yu <i>et al.</i> [72]	44.7	26.3	68.2	58.3	14674
QDTrack [35]	52.3	35.5	72.3	64.3	10790
TETer [26]	53.3	37.4	—	—	—
ByteTrack [77]	55.8	40.1	71.3	69.6	15466
SUSHI (Ours)	58.9	40.8	75.9	69.7	12076

Table 5. Validation and test set results on BDD MOT benchmark.

and we simply apply our GNNs across all of them. This naive extension of our approach already achieves significant improvements of +3.1 mIDF1 and +4.6 IDF1 over the state-of-the-art. Overall, these results further consolidate the generality of our approach and its ability to accurately track non-pedestrian classes.

6. Conclusion

We have presented SUSHI, a unified method for tracking across multiple timespans. Through our ablation studies, we have shown clear benefits from the two main features of our approach: (i) its unified nature across temporal scales, and (ii) its ability to scale to long video clips. Moreover, our benchmark results have demonstrated our model’s ability to advance state-of-the-art across highly diverse tracking scenarios, hence proving its generality.

We expect SUSHI to inspire future research by questioning the need for engineering timescale-specific solutions for tracking. Lastly, we believe SUSHI makes progress towards tackling long-term tracking, and will highlight the potential of graph hierarchies towards this end.

References

[1] R.K. Ahuja, T.L. Magnanti, and J.B. Orlin. *Network flows: Theory, algorithms and applications*. Prentice Hall, Upper Saddle River, NJ, USA, 1993. 16

[2] Jerome Berclaz, Francois Fleuret, Engin Turetken, and Pascal Fua. Multiple object tracking using k-shortest paths optimization. *IEEE TPAMI*, 33(9):1806–1819, 2011. 2, 16, 17

[3] Philipp Bergmann, Tim Meinhardt, and Laura Leal-Taixe. Tracking without bells and whistles. In *ICCV*, pages 941–951, 2019. 1, 2, 3, 6, 7, 8, 14

[4] Alex Bewley, ZongYuan Ge, Lionel Ott, Fabio Tozeto Ramos, and Ben Upcroft. Simple online and realtime tracking. *2016 IEEE International Conference on Image Processing (ICIP)*, pages 3464–3468, 2016. 1, 2

[5] Guillem Braso and Laura Leal-Taixe. Learning a neural solver for multiple object tracking. In *CVPR*, 2020. 1, 2, 3, 4, 5, 6, 7, 8, 13, 14, 15, 16

[6] A. Butt and R. Collins. Multi-target tracking by Lagrangian relaxation to min-cost network flow. *CVPR*, 2013. 2

[7] Jiarui Cai, Mingze Xu, Wei Li, Yuanjun Xiong, Wei Xia, Zhiwen Tu, and Stefano Soatto. Memot: Multi-object tracking with memory. In *Proceedings of the IEEE/CVF Conference on Computer Vision and Pattern Recognition*, pages 8090–8100, 2022. 7, 8

[8] Gregory Castañón and Lucas Finn. Multi-target tracklet stitching through network flows. In *2011 Aerospace Conference*, pages 1–7, 2011. 2, 3

[9] Peng Dai, Renliang Weng, Wongun Choi, Changshui Zhang, Zhangping He, and Wei Ding. Learning a proposal classifier for multiple object tracking. In *CVPR*, pages 2443–2452, June 2021. 1, 2, 3, 4, 5, 6, 7, 8, 14

[10] Patrick Dendorfer, Aljosa Osep, Anton Milan, Konrad Schindler, Daniel Cremers, Ian Reid, Stefan Roth, and Laura Leal-Taixé. Motchallenge: A benchmark for single-camera multiple target tracking. *International Journal of Computer Vision*, 129(4):845–881, 2021. 2, 5

[11] Patrick Dendorfer, Hamid Rezatofighi, Anton Milan, Javen Qinfeng Shi, Daniel Cremers, Ian D. Reid, Stefan Roth, Konrad Schindler, and Laura Leal-Taixé. Mot20: A benchmark for multi object tracking in crowded scenes. *ArXiv*, abs/2003.09003, 2020. 2, 5

[12] Patrick Dendorfer, Vladimir Yugay, Aljoša Ošep, and Laura Leal-Taixé. Quo vadis: Is trajectory forecasting the key towards long-term multi-object tracking? 2022. 1

[13] Zheng Ge, Songtao Liu, Feng Wang, Zeming Li, and Jian Sun. Yolox: Exceeding yolo series in 2021. *arXiv preprint arXiv:2107.08430*, 2021. 6

[14] Justin Gilmer, Samuel S Schoenholz, Patrick F Riley, Oriol Vinyals, and George E Dahl. Neural message passing for quantum chemistry. In *IEEE Int. Conf. Mach. Learn.*, pages 1263–1272. PMLR, 2017. 2

[15] Jiawei He, Zehao Huang, Naiyan Wang, and Zhaoxiang Zhang. Learnable graph matching: Incorporating graph partitioning with deep feature learning for multiple object tracking. In *CVPR*, pages 5299–5309, 2021. 1, 2, 6, 7, 14

[16] Kaiming He, Xiangyu Zhang, Shaoqing Ren, and Jian Sun. Deep residual learning for image recognition. In *CVPR*, pages 770–778, 2016. 14

[17] Andrea Hornakova, Roberto Henschel, Bodo Rosenhahn, and Paul Swoboda. Lifted disjoint paths with application in multiple object tracking. In *IEEE Int. Conf. Mach. Learn.*, pages 4364–4375. PMLR, 2020. 1, 2, 3, 4, 5, 6, 7, 8, 14

[18] Andrea Hornakova, Timo Kaiser, Paul Swoboda, Michal Rolinek, Bodo Rosenhahn, and Roberto Henschel. Making higher order mot scalable: An efficient approximate solver for lifted disjoint paths. In *ICCV*, pages 6330–6340, October 2021. 1, 2, 3, 4, 5, 7, 8, 14

[19] Chang Huang, Bo Wu, and Ramakant Nevatia. Robust object tracking by hierarchical association of detection responses. In David Forsyth, Philip Torr, and Andrew Zisserman, editors, *ECCV*, 2008. 2, 3

[20] R. Kasturi, D. Goldgof, P. Soundararajan, V. Manohar, J. Garofolo, M. Boonstra, V. Korzhova, and J. Zhang. Framework for performance evaluation for face, text and vehicle detection and tracking in video: data, metrics, and protocol. *IEEE TPAMI*, 2009. 5

[21] Diederik P Kingma and Jimmy Ba. Adam: A method for stochastic optimization. *arXiv preprint arXiv:1412.6980*, 2014. 5

[22] Laura Leal-Taixe, Cristian Canton-Ferrer, and Konrad Schindler. Learning by tracking: Siamese cnn for robust target association. In *CVPRW*, June 2016. 2

[23] Laura Leal-Taixe, Michele Fenzi, Alina Kuznetsova, Bodo Rosenhahn, and Silvio Savarese. Learning an image-based motion context for multiple people tracking. In *CVPR*, June 2014. 1

[24] Laura Leal-Taixé, Gerard Pons-Moll, and Bodo Rosenhahn. Branch-and-price global optimization for multi-view multi-target tracking. In *2012 IEEE Conference on Computer Vision and Pattern Recognition*, pages 1987–1994. IEEE, 2012. 17

[25] Jiahe Li, Xu Gao, and Tingting Jiang. Graph networks for multiple object tracking. In *Proceedings of the IEEE/CVF Winter Conference on Applications of Computer Vision (WACV)*, March 2020. 2

[26] Siyuan Li, Martin Danelljan, Henghui Ding, Thomas E Huang, and Fisher Yu. Tracking every thing in the wild. In *European Conference on Computer Vision*, pages 498–515. Springer, 2022. 8

[27] Shuai Li, Yu Kong, and Hamid Rezatofighi. Learning of global objective for network flow in multi-object tracking. In *Proceedings of the IEEE/CVF Conference on Computer Vision and Pattern Recognition*, pages 8855–8865, 2022. 7, 8, 14

[28] Wei Li, Rui Zhao, Tong Xiao, and Xiaogang Wang. Deep-reid: Deep filter pairing neural network for person re-identification. In *2014 IEEE Conference on Computer Vision and Pattern Recognition*, pages 152–159, 2014. 13, 14

[29] Tsung-Yi Lin, Priya Goyal, Ross Girshick, Kaiming He, and Piotr Dollar. Focal loss for dense object detection. In *ICCV*, 2017. 5

[30] Qiankun Liu, Qi Chu, Bin Liu, and Nenghai Yu. Gsm: Graph similarity model for multi-object tracking. In *IJCAI*, pages 530–536, 2020. 2

[31] Jonathon Luiten, Aljosa Osep, Patrick Dendorfer, Philip Torr, Andreas Geiger, Laura Leal-Taixé, and Bastian Leibe. Hota: A higher order metric for evaluating multi-object tracking. *IJCV*, 129(2):548–578, 2021. 5

[32] Tim Meinhardt, Alexander Kirillov, Laura Leal-Taixé, and Christoph Feichtenhofer. Trackformer: Multi-object tracking with transformers. In *IEEE Conf. Comput. Vis. Pattern Recog.*, 2022. 1, 2, 3, 7, 8

[33] Anton Milan, S. Hamid Rezatofighi, Anthony Dick, Ian Reid, and Konrad Schindler. Online multi-target tracking using recurrent neural networks. In *Proceedings of the Thirty-First AAAI Conference on Artificial Intelligence*, 2017. 2

[34] Xingang Pan, Ping Luo, Jianping Shi, and Xiaoou Tang. Two at once: Enhancing learning and generalization capacities via ibn-net. In *ECCV*, pages 464–479, 2018. 14

[35] Jiangmiao Pang, Linlu Qiu, Xia Li, Haofeng Chen, Qi Li, Trevor Darrell, and Fisher Yu. Quasi-dense similarity learning for multiple object tracking. In *CVPR*, pages 164–173, 2021. 1, 2, 8

[36] Jiangmiao Pang, Linlu Qiu, Xia Li, Haofeng Chen, Qi Li, Trevor Darrell, and Fisher Yu. Quasi-dense similarity learning for multiple object tracking. In *CVPR*, pages 164–173, June 2021. 7

[37] Hamed Pirsiavash, Deva Ramanan, and Charless C. Fowlkes. Globally-optimal greedy algorithms for tracking a variable number of objects. In *CVPR*, pages 1201–1208, 2011. 17

[38] Jérôme Revaud, Philippe Weinzaepfel, Zaïd Harchaoui, and Cordelia Schmid. Deepmatching: Hierarchical deformable dense matching. *International Journal of Computer Vision*, 120:300–323, 2016. 1

[39] Hamid Rezatofighi, Nathan Tsoi, JunYoung Gwak, Amir Sadeghian, Ian Reid, and Silvio Savarese. Generalized intersection over union: A metric and a loss for bounding box regression. In *CVPR*, pages 658–666, 2019. 5, 15

[40] Ergys Ristani, Francesco Solera, Roger Zou, Rita Cucchiara, and Carlo Tomasi. Performance measures and a data set for multi-target, multi-camera tracking. In *Eur. Conf. Comput. Vis. Worksh.*, pages 17–35. Springer, 2016. 5

[41] E. Ristani, F. Solera, R. S. Zou, R. Cucchiara, and C. Tomasi. Performance measures and a data set for multi-target, multi-camera tracking. *Eur. Conf. Comput. Vis. Worksh.*, 2016. 13

[42] Ergys Ristani, Francesco Solera, Roger S. Zou, Rita Cucchiara, and Carlo Tomasi. Performance measures and a data set for multi-target, multi-camera tracking. In *ECCV Workshops*, 2016. 14

[43] Ergys Ristani and Carlo Tomasi. Features for multi-target multi-camera tracking and re-identification. In *2018 IEEE/CVF Conference on Computer Vision and Pattern Recognition*, pages 6036–6046, 2018. 1

[44] Ergys Ristani and Carlo Tomasi. Features for multi-target multi-camera tracking and re-identification. In *CVPR*, June 2018. 2

[45] Alexandre Robicquet, Amir Sadeghian, Alexandre Alahi, and Silvio Savarese. Learning social etiquette: Human trajectory understanding in crowded scenes. In *ECCV*, 2016. 1

[46] Amir Sadeghian, Alexandre Alahi, and Silvio Savarese. Tracking the untrackable: Learning to track multiple cues with long-term dependencies. In *ICCV*, Oct 2017. 2

[47] Franco Scarselli, Marco Gori, Ah Chung Tsoi, Markus Hagenbuchner, and Gabriele Monfardini. The graph neural network model. *IEEE Transactions on Neural Networks*, 20(1):61–80, 2009. 2

[48] Jeany Son, Mooyeon Baek, Minsu Cho, and Bohyung Han. Multi-object tracking with quadruplet convolutional neural networks. In *CVPR*, July 2017. 1, 2

[49] Daniel Stadler and Jurgen Beyerer. Improving multiple pedestrian tracking by track management and occlusion handling. In *CVPR*, pages 10958–10967, June 2021. 14

[50] Peize Sun, Jinkun Cao, Yi Jiang, Zehuan Yuan, Song Bai, Kris Kitani, and Ping Luo. Dancetrack: Multi-object tracking in uniform appearance and diverse motion. In *CVPR*, 2022. 2, 5

[51] Valteri Takala and Matti Pietikainen. Multi-object tracking using color, texture and motion. In *2007 IEEE Conference on Computer Vision and Pattern Recognition*, pages 1–7, 2007. 2

[52] Siyu Tang, Bjoern Andres, Mykhaylo Andriluka, and Bernt Schiele. Subgraph decomposition for multi-target tracking. In *Proceedings of the IEEE Conference on Computer Vision and Pattern Recognition (CVPR)*, June 2015. 1, 2

[53] Siyu Tang, Mykhaylo Andriluka, Bjoern Andres, and Bernt Schiele. Multiple people tracking by lifted multicut and person re-identification. In *CVPR*, July 2017. 1, 2

[54] Siyu Tang, Mykhaylo Andriluka, Bjoern Andres, and Bernt Schiele. Multiple people tracking by lifted multicut and person re-identification. In *2017 IEEE Conference on Computer Vision and Pattern Recognition (CVPR)*, pages 3701–3710, Washington, DC, USA, July 2017. IEEE Computer Society. 17

[55] Pavel Tokmakov, Jie Li, Wolfram Burgard, and Adrien Gaidon. Learning to track with object permanence. In *ICCV*, pages 10860–10869, October 2021. 1, 2, 7

[56] Jack Valmadre, Alex Bewley, Jonathan Huang, Chen Sun, Cristian Sminchisescu, and Cordelia Schmid. Local metrics for multi-object tracking. *arXiv preprint arXiv:2104.02631*, 2021. 13

[57] Qiang Wang, Yun Zheng, Pan Pan, and Yinghui Xu. Multiple object tracking with correlation learning. In *CVPR*, pages 3876–3886, 2021. 7, 8

[58] Shuai Wang, Hao Sheng, Yang Zhang, Yubin Wu, and Zhang Xiong. A general recurrent tracking framework without real data. In *ICCV*, pages 13219–13228, October 2021. 7

[59] Yongxin Wang, Kris Kitani, and Xinshuo Weng. Joint object detection and multi-object tracking with graph neural networks. In *IEEE Int. Conf. Robotics and Autom.*, pages 13708–13715. IEEE, 2021. 8

[60] Zhongdao Wang, Liang Zheng, Yixuan Liu, and Shengjin Wang. Towards real-time multi-object tracking. *The European Conference on Computer Vision (ECCV)*, 2020. 1, 2

[61] Longhui Wei, Shiliang Zhang, Wen Gao, and Qi Tian. Person transfer gan to bridge domain gap for person re-identification. In *2018 IEEE/CVF Conference on Computer Vision and Pattern Recognition*, pages 79–88, 2018. [13](#), [14](#)

[62] Longyin Wen, Wenbo Li, Junjie Yan, Zhen Lei, Dong Yi, and Stan Z. Li. Multiple target tracking based on undirected hierarchical relation hypergraph. In *Proceedings of the IEEE Conference on Computer Vision and Pattern Recognition (CVPR)*, June 2014. [2](#), [3](#)

[63] Xinshuo Weng, Yongxin Wang, Yunze Man, and Kris M. Kitani. Gnn3dmot: Graph neural network for 3d multi-object tracking with 2d-3d multi-feature learning. In *Proceedings of the IEEE/CVF Conference on Computer Vision and Pattern Recognition (CVPR)*, June 2020. [2](#)

[64] Nicolai Wojke, Alex Bewley, and Dietrich Paulus. Simple online and realtime tracking with a deep association metric. In *ICIP*, pages 3645–3649, 2017. [1](#), [2](#), [3](#)

[65] Sanghyun Woo, Kwanyong Park, Seoung Wug Oh, In So Kweon, and Joon-Young Lee. Tracking by associating clips. In *ECCV*, October 2022. [3](#)

[66] Jialian Wu, Jiale Cao, Liangchen Song, Yu Wang, Ming Yang, and Junsong Yuan. Track to detect and segment: An online multi-object tracker. In *CVPR*, 2021. [8](#)

[67] Jiarui Xu, Yue Cao, Zheng Zhang, and Han Hu. Spatial-temporal relation networks for multi-object tracking. In *ICCV*, October 2019. [2](#)

[68] Yuanlu Xu, Xiaobai Liu, Yang Liu, and Song-Chun Zhu. Multi-view people tracking via hierarchical trajectory composition. In *Proceedings of the IEEE Conference on Computer Vision and Pattern Recognition (CVPR)*, June 2016. [2](#), [3](#)

[69] Yihong Xu, Aljosa Osep, Yutong Ban, Radu Horaud, Laura Leal-Taixe, and Xavier Alameda-Pineda. How to train your deep multi-object tracker. In *CVPR*, June 2020. [1](#)

[70] Bin Yan, Yi Jiang, Peize Sun, Dong Wang, Zehuan Yuan, Ping Luo, and Huchuan Lu. Towards grand unification of object tracking. In *European Conference on Computer Vision*, pages 733–751. Springer, 2022. [7](#), [8](#)

[71] Bo Yang and Ram Nevatia. An online learned crf model for multi-target tracking. In *2012 IEEE Conference on Computer Vision and Pattern Recognition*, pages 2034–2041, 2012. [2](#)

[72] Fisher Yu, Haofeng Chen, Xin Wang, Wenqi Xian, Yingying Chen, Fangchen Liu, Vashisht Madhavan, and Trevor Darrell. Bdd100k: A diverse driving dataset for heterogeneous multitask learning. In *Proceedings of the IEEE/CVF conference on computer vision and pattern recognition*, pages 2636–2645, 2020. [2](#), [5](#), [8](#)

[73] Amir Roshan Zamir, Afshin Dehghan, and Mubarak Shah. Gmcp-tracker: Global multi-object tracking using generalized minimum clique graphs. In *ECCV*, pages 343–356. Springer, 2012. [2](#)

[74] Fangao Zeng, Bin Dong, Yuang Zhang, Tiancai Wang, Xiangyu Zhang, and Yichen Wei. Motr: End-to-end multiple-object tracking with transformer. In *European Conference on Computer Vision (ECCV)*, 2022. [2](#)

[75] Fangao Zeng, Bin Dong, Yuang Zhang, Tiancai Wang, Xiangyu Zhang, and Yichen Wei. Motr: End-to-end multiple-object tracking with transformer. In *European Conference on Computer Vision*, pages 659–675. Springer, 2022. [7](#), [8](#)

[76] Li Zhang, Yuan Li, and Ramakant Nevatia. Global data association for multi-object tracking using network flows. In *CVPR*, 2008. [2](#), [3](#), [17](#)

[77] Yifu Zhang, Peize Sun, Yi Jiang, Dongdong Yu, Zehuan Yuan, Ping Luo, Wenyu Liu, and Xinggang Wang. Byte-track: Multi-object tracking by associating every detection box. *arXiv preprint arXiv:2110.06864*, 2021. [1](#), [2](#), [6](#), [7](#), [8](#), [14](#)

[78] Yifu Zhang, Chunyu Wang, Xinggang Wang, Wenjun Zeng, and Wenyu Liu. Fairmot: On the fairness of detection and re-identification in multiple object tracking. *IJCV*, 129(11):3069–3087, 2021. [1](#), [2](#), [7](#), [8](#)

[79] Liang Zheng, Liyue Shen, Lu Tian, Shengjin Wang, Jingdong Wang, and Qi Tian. Scalable person re-identification: A benchmark. In *2015 IEEE International Conference on Computer Vision (ICCV)*, pages 1116–1124, 2015. [13](#), [14](#)

[80] Xingyi Zhou, Vladlen Koltun, and Philipp Krähenbühl. Tracking objects as points. In *ECCV*, pages 474–490. Springer, 2020. [1](#), [2](#), [8](#), [14](#)

[81] Xingyi Zhou, Tianwei Yin, Vladlen Koltun, and Philipp Krähenbühl. Global tracking transformers. In *Proceedings of the IEEE/CVF Conference on Computer Vision and Pattern Recognition*, pages 8771–8780, 2022. [2](#), [5](#), [7](#), [8](#)

Supplementary Material

In this supplementary material, we provide (i) additional ablation studies and extended benchmark comparisons (Sec. A) (ii) further details about our method (Sec. B) and (iii) an additional discussion (Sec. C).

A. Additional Experiments

A.1. Analysis on maximum temporal edge distance

SUSHI is capable of processing clips of arbitrary length but we construct graphs with a maximum temporal edge distance of 150 frames as we experimentally found that this covers the majority of long-term association cases. In Figure 5, we visualize the maximum frame gaps within trajectories as a histogram on the MOT17 training set when public detections are associated by an oracle. A vast majority of the trajectories (more than 98%) can be constructed without an error with a clip size of 150 frames, and gains diminish for higher frame distances. In addition, we report the cross-validation scores obtained by our model with different maximum temporal edge distance parameters in Figure 6. We observe that processing larger clips improves the results up to 150 frames but scores stagnate after this point. Overall, we experimentally found 150 frames to be a good trade-off between performance, memory requirements, and training speed.

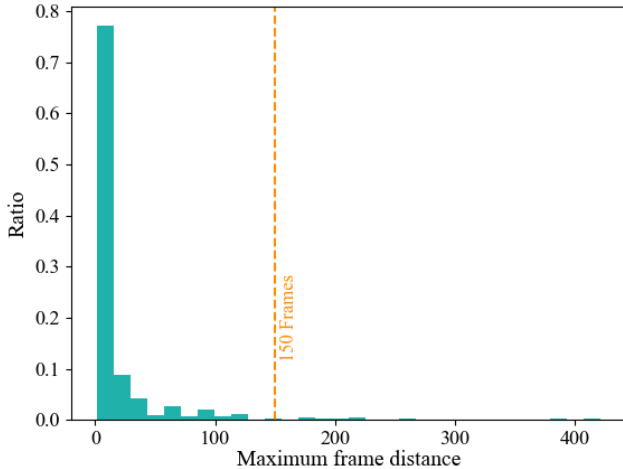


Figure 5. Histogram of maximum frame distance of trajectories constructed by an oracle on MOT17 training set.

A.2. Memory requirement and hierarchy levels

Our graph hierarchy significantly reduces the number of edges in a graph and further mitigates the label imbalance between correct and incorrect trajectory hypotheses, as we showed in the Figure 4a of the main paper. Consequently, having fewer edges in graphs results in lower

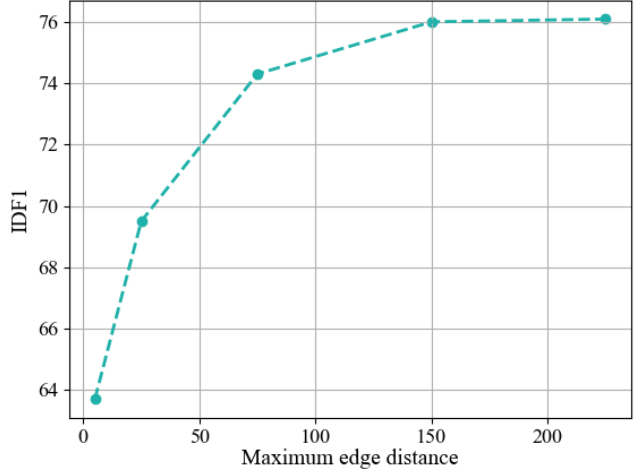


Figure 6. Scores reached by our model with different maximum temporal edge distance parameters.

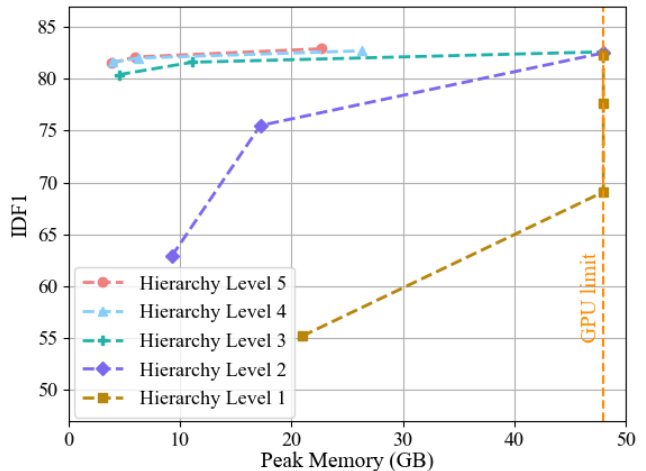


Figure 7. Upper bound IDF1 score with respect to peak training memory. GPU limit is given for a single Quadro RTX 8000 GPU.

memory requirements to train models. We further quantify this phenomenon by reporting the upper bound IDF1 score and peak training memory with a varying number of hierarchical levels in Figure 7. Each data point is obtained by setting different K values while pruning during graph construction. We observe that our hierarchy drastically reduces the peak training memory requirements. Specifically, a non-hierarchical configuration with a single level achieves 55 IDF1 with approximately 20 GB memory, while the models with four and five levels reach 81 IDF1 with one-fourth of the memory requirement.

A.3. Temporal analysis of tracking performance

We perform a temporal analysis on our model with a different number of hierarchy levels (SUSHI blocks) as well

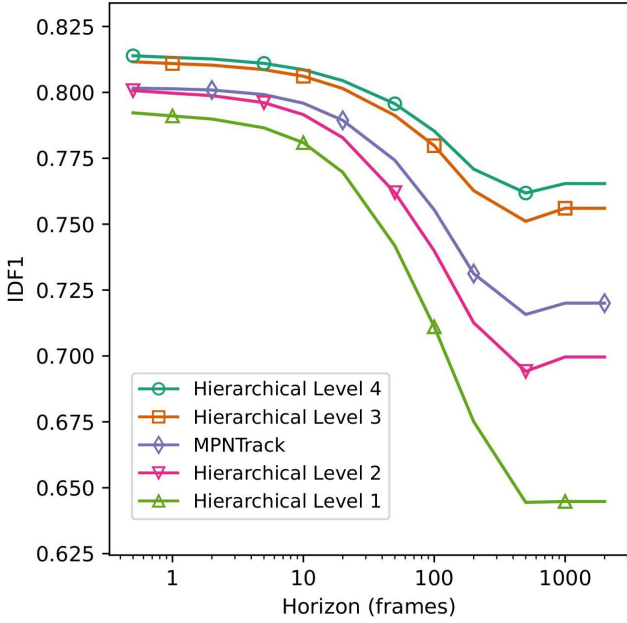


Figure 8. Temporal analysis of tracking performance with Local-MOT.

#	Strategy	Clip sizes	IDF1 ↑	HOTA ↑	MOTA ↑
1	Balanced (Ours)	5-25-75-150	76.0	65.8	68.6
2	Short Term	2-6-30-150	73.0	63.7	68.2
3	Short Term	5-10-30-150	74.0	64.4	68.0
4	Long Term	25-75-150-150	66.2	59.1	60.6
5	Long Term	50-150-150-150	59.6	54.3	48.8

Table 6. Clip sizes partition configuration.

as MPNTrack to outline how different aspects of tracking benefit from our hierarchy in Figure 8. For this, we use LocalMOT [56] which restricts IDF1 computation to a finite temporal horizon and breaks down how a tracker’s performance evolves from short-term to long-term. We observe monotonic improvements in association performance across all temporal horizons with models with more hierarchy levels. Especially in large temporal horizons, corresponding to long-term association cases, we observe a significant performance increase compared to MPNTrack, which indicates that we especially improve long-term tracking with our hierarchical method.

A.4. Clip sizes partition configuration

Our graph hierarchies are based on a recursive partition of a video into clips. In order to get the most out of our proposed graph hierarchies, their corresponding clip length configurations needs to be carefully designed. Intuitively, clips should grow in a progressive manner, so that the tracklet-merging workload is evenly distributed among

Appearance representation	IDF1 ↑	HOTA ↑	MOTA ↑
Closest obj. detection	70.8	62.4	68.0
Track-Max	74.5	64.8	68.3
Track-Avg	76.0	65.8	68.6

Table 7. Effect of different appearance representations.

ReID model	Training data	IDF1 ↑	HOTA ↑	MOTA ↑
ResNet50	[28, 41, 79]	76.7	66.1	68.7
ResNet50-IBN	[61]	76.0	65.8	68.3

Table 8. Effect of using [5]’s original reID model (ResNet50 trained on 3 datasets) vs ours (ResNet50-IBN trained on a single dataset).

hierarchy levels. In Tab. 6, we explore several variations of our best configuration. All variations consist of 4 levels operating over a clip with 150 frames. In rows #2 and #3, the small windows in the early layers focus mostly on short-term associations, and the final merging of tracklets is relatively aggressive. The full potential of the hierarchy cannot be exploited in this configuration: later levels operate over relatively short tracklets and therefore have less robust association cues. At the same time, they attempt to merge tracklets from an increased number of clips, thereby increasing the complexity of their task. In contrast, rows #4 and #5 start from large clips and quickly consider tracklets spanning over all frames at once. Since at the first level we cannot compute tracklet-level features, *e.g.* based on motion, the model is more prone to errors. These errors are then propagated to later layers and cannot be recovered. As we can see in row #1, our configuration yields better results, highlighting the importance of following a more balanced merging sequence.

A.5. Appearance features

As we observed in Figure 4c of the main paper, appearance plays the largest role among all feature sources. In Table 7, we further investigate alternative ways to encode track-level appearance. Notably, using appearance embeddings from the closest detections among tracklets instead of average tracklet-level embeddings yields a significant decrease of over 5 IDF1. This highlights the importance of exploiting the entire set of appearance embeddings over tracklets. Lastly, aggregating embeddings with a max operation, instead of averaging them, yields a modest decrease of 1.5 IDF1.

A.6. Different ReID model

Our method inherits the GNN architecture of MPN-Track [5], but we use a different reID model as their model is trained on a retracted dataset. Specifically, instead of ResNet50 [16], we use a ResNet50-IBN [34] variant, following [9], pretrained on MSMT17 [61], an extension of Market-1501². We do this in an attempt to match the reID performance of [5], without resorting to withdrawn datasets. Note that MPNTrack [5] trained its model on three different datasets: Market-1501 [79], CUHK03 [28], and the currently retracted DukeMTC [42]. Instead, we use a single public dataset [61]. In Table 8, we report MOT17 cross-validation results using our reID model and the one used by [5]. We observe that our reID model performs moderately worse. Despite using a clearly worse reID model, our overall approach still outperforms MPNTrack [5] by 6.9 IDF1 on the MOT17 test set. These results further highlight that our improvements are due to our main contributions.

A.7. Extended benchmark results on MOTChallenge with public detections

Method	Det Ref.	IDF1 ↑	HOTA ↑	MOTA ↑	ID Sw. ↓
MOT17 - Public					
Tracktor [3]	Tracktor	55.1	44.8	56.3	1987
LPT [27]	Tracktor	57.7	–	57.3	1424
MPNTrack [5]	Tracktor	61.7	49.0	58.8	1185
Lif_T [17]	Tracktor	65.6	51.3	60.5	1189
ApLift [18]	Tracktor	65.6	51.1	60.5	1709
GMT [15]	Tracktor	65.9	51.2	60.2	1675
LPC_MOT [9]	Tracktor	66.8	51.5	59.0	1122
SUSHI (Ours)	Tracktor	68.6	53.0	62.2	1062
CenterTrack [80]	CenterTrack	59.6	48.2	61.5	2583
TMOH [49]	TMOH	62.8	50.4	62.1	1897
ByteTrack [77]	ByteTrack	70.0	56.1	67.4	1331
SUSHI (Ours)	ByteTrack	73.4	58.5	68.4	1033
MOT20 - Public					
Tracktor [3]	Tracktor	52.7	42.1	52.6	1648
LPT [27]	Tracktor	53.5	–	57.9	1827
ApLift [18]	Tracktor	56.5	46.6	58.9	2241
MPNTrack [5]	Tracktor	59.1	46.8	57.6	1210
LPC_MOT [9]	Tracktor	62.5	49.0	56.3	1562
SUSHI (Ours)	Tracktor	68.2	53.4	61.6	1078
TMOH [49]	TMOH	61.2	48.9	60.1	2342
ByteTrack [77]	ByteTrack	70.2	56.4	67.0	680
SUSHI (Ours)	ByteTrack	73.3	58.4	67.2	601

Table 9. Extended test set results on MOTChallenge under public setting with additional refinement strategies. Det. Ref. denotes the public detection refinement strategy.

MOTChallenge presents a public setting in which ob-

²The model is publicly available at https://github.com/JDAI-CV/fast-reid/blob/master/MODEL_ZOO.md

ject detections are provided to emphasize data association performance during evaluation. In the public setting, it is a common practice among published methods to refine the public detections of the MOTChallenge [3,5,9,15,17,18,27,49,77,80] with local tracking schemes that enable adding additional boxes [3,49,77,80]. These processing schemes have a large impact on the detection quality and the overall tracking scores.

In the main paper, we reported public setting results with the Tracktor-based refinement as it is the most commonly used one. To compare our method with a wider range of trackers, in Table 9 we report results with an additional processing scheme and show further improvements over methods using alternative preprocessing schemes as well. Specifically, we significantly outperform the state-of-the-art by +3.4 IDF1 and +2.4 HOTA on MOT17 and +3.1 IDF1 and +2.0 HOTA on MOT20 while using the same set of detections.

B. Additional Details about SUSHI

B.1. Edge association cues

As explained in Section 4.2, we feed an initial vector of concatenated pairwise association features to a light-weight multi-layer perception MLP_{edge} to compute input edge embeddings in each SUSHI block. Specifically, we obtain these features from tracklets and embed information about time distance, reID-based appearance similarity, spatial and motion-based proximity between two nodes.

Time and position information. Similarly to [5], we encode the relative position and time distance among nodes as initial edge features. We naturally extend this notion from single detections to tracks by considering the closest detections in time for each pair of tracks. Formally, given the box coordinate and timestamps of two tracklets T_u and T_v , defined as $u = \{(x_i, y_i, w_i, h_i, t_i)\}_{i=u_1}^{u_{n_u}}$ and $v = \{(x_i, y_i, w_i, h_i, t_i)\}_{i=v_1}^{v_{n_v}}$, assuming $t_{u_{n_u}} < t_{v_1}$ i.e. T_u ends before T_v starts, we compute the following position features:

$$\left(\frac{2(x_{n_u} - x_{v_1})}{h_{u_{n_u}} + h_{v_1}}, \frac{2(y_{u_{n_u}} - y_{v_1})}{h_{u_{n_u}} + h_{v_1}}, \log \frac{w_{u_{n_u}}}{w_1}, \log \frac{h_{u_{n_u}}}{h_1^v} \right)$$

and we naturally compute time difference as $t_{u_{n_u}} - t_{v_1}$.

Appearance Representation. For every object detection $o_i \in \mathcal{O}$ we obtain embedding ρ_i representing its appearance by feeding its image patch to a pretrained convolutional network, $\rho_i = CNN_{app}(a_i)$. Intuitively, while single embeddings can be affected by motion blur or sudden illumination changes, a representation summarizing the entire set can be more robust to such phenomena. Hence, we use the euclidean distance among averaged embeddings of tracks as an appearance similarity term $\|\rho_{avg}^u - \rho_{avg}^v\|_2$.

Motion consistency. Trajectories are expected to be continuous in the spatio-temporal domain. We utilize this cue by defining an additional edge feature encoding the motion consistency of each pair of tracklets. Given two tracklets T_u and T_v , we estimate their respective velocities in the pixel domain as v_u and v_v , respectively. Assuming again $t_{n_u} < t_{v_1}$, we use the estimated velocities to forward propagate u 's last position and backward propagate v 's first position until their middle time point $t^{\text{mid}} := (t_{v_1} - t_{u_{n_u}})/2$, to minimize the prediction horizon from each track. Formally, we compute $\text{pos}_{u \rightarrow v}^{\text{fwd}} := b_{u_{n_u}} + t^{\text{mid}} v_u$ and $\text{pos}_{v \rightarrow u}^{\text{bwd}} := b_{v_1} - t^{\text{mid}} v_v$, to obtain the edge feature $\text{GIoU}(\text{pos}_{u \rightarrow v}^{\text{fwd}}, \text{pos}_{v \rightarrow u}^{\text{bwd}})$, where GIoU denotes the Generalized Intersection over Union score [39]. We choose the GIoU score over the commonly used Intersection over Union because the former still provides a meaningful signal whenever two boxes do not intersect.

B.2. Additional implementation details

Clip stitching. As explained in the main paper, SUSHI operates over video clips of 150 frames. To obtain trajectories over video sequences of arbitrary length, we process videos in an overlapping sliding window fashion. More specifically, we set the overlap among windows to be 75 frames and therefore process videos into clips with corresponding frame intervals (1, 150), (75, 225), (150, 300), and so on. To stitch trajectories in overlapping windows, we use a simple bipartite matching-based algorithm. Let \mathcal{T}_A and \mathcal{T}_B represent the sets of tracks in two overlapping windows, respectively, restricted over the frame interval in which they overlap. Since all trajectories in \mathcal{T}_A and \mathcal{T}_B are built over the same initial set of object detections, for every pair of trajectories $T_A \in \mathcal{T}_A$ and $T_B \in \mathcal{T}_B$, we can consider their IoU *i.e.* the ratio of boxes that they share in common:

$$\text{IoU}(T_A, T_B) = \frac{\#(T_A \cap T_B)}{\#(T_A \cup T_B)}$$

Note that whenever trajectory predictions among the two clips are *consistent*, their IoU will be 1, and whenever they don't share any boxes, it will be 0. Once we have computed the IoU between each pair of trajectories $T_A \in \mathcal{T}_A$ and $T_B \in \mathcal{T}_B$, we define their pairwise cost as:

$$c(T_A, T_B) := \begin{cases} 1 - \text{IoU}(T_A, T_B) & \text{if } \#(T_A \cap T_B) > 0 \\ \infty & \text{otherwise.} \end{cases}$$

where the second clause prevents non-overlapping tracks from being matched. Using this formulation, we obtain the min-cost bipartite matching between \mathcal{T}_A and \mathcal{T}_B , and assign the same identity to matched trajectories.

Edge pruning. As mentioned in Section 5.2 of the main paper, we define the set of edges of each graph in our hierarchy by considering for each node, its top K nearest neighbors

(KNNs) according to a position, appearance and motion-based similarity measure. Making graphs sparse with KNN-based edge filtering helps to reduce the number of edges, and therefore computational burden, as well as improving the edge label imbalance. Intuitively, edges between nodes with drastically different appearance or infeasible motion can be discarded early. However, there is a tradeoff: low values of K might also discard edges belonging to ground truth trajectories in case of noisy features. Notably, single monolithic graphs such as MPNTrack's [5] require high values of K to achieve good performance, while in our framework consisting of relatively smaller graphs $K = 15$ suffices, yielding significantly better label distribution.

Choosing the right distance metric to prune edges is crucial for the overall success of this strategy. Intuitively, nodes that are close should be likely to belong to the same trajectory. While MPNTrack relied solely on the distance among appearance embeddings, we take advantage of two features of our hierarchy: i) in lower hierarchy levels, nodes within the same trajectory tend to be very close in space and time ii) in higher levels, we have motion information, which can help us determine physically unreasonable connections. To exploit these facts, for graphs in the first level of our hierarchy, we simply use the coordinate-based distance between each pair of tracks as a similarity measure. In subsequent levels, for each pair of tracklets T_u and T_v we define their distance for edge pruning as: $d(T_u, T_v) := \lambda d_{\text{app}}(T_u, T_v) + (1 - \lambda) d_{\text{motion}}(T_u, T_v)$, where d_{app} is the euclidean distance of their appearance embeddings, and d_{motion} is 1 minus their GIoU score. We empirically set $\lambda = 0.05$.

B.3. Message passing network architecture

Time-aware neural message passing updates As explained in Section 4 of the main paper, at the core of our SUSHI blocks there is a message passing GNN that, given a graph at each level of our hierarchy, takes as input its initial set of node and edge embeddings, and produces new embeddings encoding high-order contextual information, that we later use for edge classification. We now explain them in detail. Formally, for each graph $G^l = (V^l, E^l)$ at level l in our hierarchy, we consider embeddings $h_v^{(0)} \in \mathbb{R}^{d_V}$ and $h_{(u,w)}^{(0)} \in \mathbb{R}^{d_E}$ for every node $v \in V^l$ and edge $(u, w) \in E^l$, with d_V and d_E being their respective dimension. For a fixed number of steps, $s = 1, \dots, S$ and each node $v \in V^l$

and edge $(u, v) \in E^l$ we do:

$$h_{(u,v)}^{(s)} = \text{MLP}_{\text{edge}}^l \left(\left[h_u^{(s-1)}, \bar{h}_{(u,v)}^{(s-1)}, h_v^{(s-1)} \right] \right) \quad (1)$$

$$m_{u \rightarrow v}^{(s)} = \begin{cases} \text{MLP}_{\text{past}}^l \left([h_u^{(s-1)}, \bar{h}_{(u,v)}^{(s)}, h_v^{(s-1)}] \right) \text{ if } t_u^{\text{end}} < t_v^{\text{start}} \\ \text{MLP}_{\text{future}}^l \left([h_u^{(s-1)}, \bar{h}_{(u,v)}^{(s)}, h_v^{(s-1)}] \right) \text{ else.} \end{cases} \quad (2)$$

$$h_v^{(s)} = \text{MLP}_{\text{node}}^l \left(\left[\sum_{u | t_u^{\text{end}} < t_v^{\text{start}}} m_{u \rightarrow v}^{(s)}, \sum_{u | t_u^{\text{start}} < t_v^{\text{end}}} m_{u \rightarrow v}^{(s)} \right] \right) \quad (3)$$

where MLP_*^l denote multi-layer perceptrons that are shared across the entire hierarchy level l , $[*, *]$ denotes concatenation, $\bar{h}_{(u,v)}^{(s)} := [h_{(u,v)}^{(s)}, h_{(u,v)}^{(0)}]$ and t_u^{start} (resp. t_u^{end}) denotes the first (resp. last) timestamp of the tracklet associated to node $u \in V^l$. Intuitively, edges are updated by combining their incident nodes' information. Then nodes are updated by separately aggregating over embeddings from their neighboring incident edges in future and past frames separately, to account for the time directionality. These updates follow the message-passing scheme in [5] and, despite relying on a set of lightweight multi-layer perceptrons, they yield embeddings enabling high-accuracy edge classification.

Detailed MLP architectures. Our SUSHI blocks consist of the MLPs defined above for neural message passing, our edge classifier $\text{MLP}_{\text{class}}$, and an additional MLP used to initialize edge embeddings from their initial features, denoted as $\text{MLP}_{\text{edge}}^{\text{init}}$. All of their exact architectures are detailed in Figure 9. We do not count learnable per-level embeddings due to their negligible cost. Overall, our architecture not including the ResNet50-IBN reID model, has a total of approximately 22K parameters, which is notably small for deep learning standards.

B.4. Rounding edge predictions via linear programming

As mentioned in Section 4.2, given a set of edge predictions $y_{(u,v) \in E}^{\text{pred}}$ over a graph $G = (V, E)$, we use a linear programming-based algorithm to obtain a new set of tracklets following [5]. We now explain this algorithm in detail: we first look at the problem constraints and then provide the final algorithm used to enforce them.

Flow conservation-type constraints. Recall that edge predictions aim to approximate the set of edge labels $\{y_{(u,v)}^{\text{pred}}\}_{(u,v) \in E}$. Further recall that these labels are defined by considering the set of edges corresponding to trajectory-paths in the graph. Specifically, given a time-ordered track $T_k = \{o_{k_i}\}_{i=1}^{n_k}$ with $t_{k_i} < t_{k_{i+1}}$, we consider its corresponding path in G given by its edges

$E(T_k) := \{(o_{k_1}, o_{k_2}), \dots, (o_{k_{n_k-1}}, o_{k_{n_k}})\}$, and hence define, for each $(o_i, o_j) \in E$:

$$y_{(o_i, o_j)} = \begin{cases} 1 & \text{if } \exists T_k \in \mathcal{T}^* \text{ s.t. } (o_i, o_j) \in E(T_k) \\ 0 & \text{otherwise} \end{cases} \quad (4)$$

Now, notice that since each node (*i.e.* object detection) can belong to at most one trajectory, edge labels need to satisfy the following constraints:

$$\sum_{(o_j, o_i) \in E \text{ s.t. } t_i > t_j} y_{(o_j, o_i)} \leq 1 \quad \forall o_i \in V \quad (5)$$

$$\sum_{(o_i, o_k) \in E \text{ s.t. } t_i < t_k} y_{(o_i, o_k)} \leq 1 \quad \forall o_i \in V \quad (6)$$

Since y 's are binary, these constraints state that each node should have, at most, one incident edge labeled as 1 connecting it to a future (resp. past) node, and they are analogous to the conservation constraints used in network flows problems [1].

Projection algorithm. The set of edge predictions, $\{y_{(u,v)}^{\text{pred}}\}_{(u,v) \in E}$ produced by our GNN already satisfies approximately 99% of the aforementioned constraints [5] by simply thresholding them at 0.5. In general, however, having unsatisfied constraints makes it ambiguous to determine the trajectory of an object. In other words, if a node has two positive-labeled edges connecting it to nodes in future locations, it becomes unclear which edge should be selected to form its trajectory. To address these cases, we consider the subgraph of nodes and edges that, after thresholding, violate inequalities 5 or 6, denoted as \bar{V} and \bar{E} , respectively, and obtain the closest feasible binary solution y^{round} to our predictions y^{pred} by solving the following integer linear program:

$$\begin{aligned} \min_{y^{\text{round}}} \quad & y^{\text{round}} (1 - 2y^{\text{pred}}) \\ \text{subject to} \quad & y^{\text{round}} \text{ satisfying ineq. 5 and 6 for all nodes in } \bar{V} \\ & y_{(u,v)}^{\text{round}} \in \{0, 1\} \quad \forall (u, v) \in \bar{E} \end{aligned} \quad (7)$$

where we index both y^{round} and y^{pred} indexed for all edges $(u, v) \in \bar{E}$. Note that, since y^{round} is binary, this objective is equivalent to minimizing the euclidean distance $\|y^{\text{round}} - y^{\text{pred}}\|_2$. Moreover, it can be shown that the constraint matrix in 7 is unimodular, and hence solving the linear relaxation of the problem yields a global integer optimum [2]. Overall, Eq. 7 can be very efficiently solved with off-the-shelf linear programming solvers as the graph over which it is defined has very few nodes and edges due to a high percentage of feasible edge predictions produced by our network that can be directly thresholded.

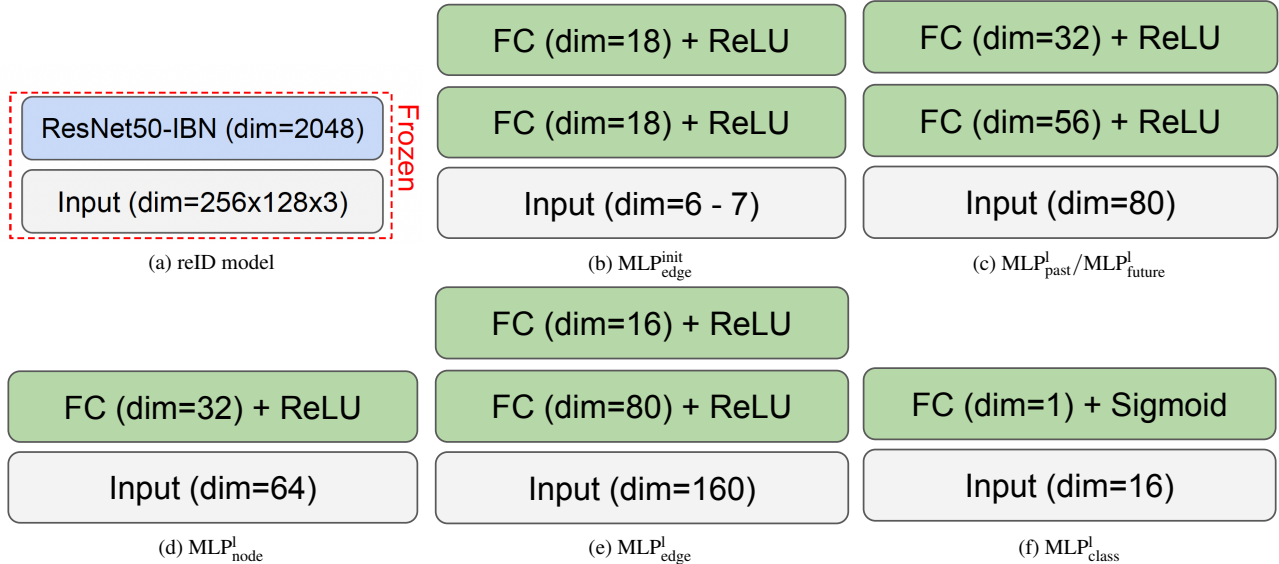


Figure 9. Detailed architectures of all components of our model.

C. Offline Tracking

We note that our tracker works in an offline manner. That is, it performs data association by considering batches of frames. This is in contrast to frame-by-frame online trackers, which process videos sequentially by only considering current and past frames at each step.

Offline approaches can search for global solutions over the batch of frames that they consider. Therefore, they are often more robust than their online counterparts, and they are preferred for a wide range of applications including video analysis, video editing, and semi-automated video labeling. Thus, offline multi-object tracking has been an active area of research for decades [2, 24, 37, 54, 76], and progress in the field is very much of interest to the community.